Picosecond polarised fluorescence studies of oxazine 4 motion and order in nematic and isotropic phases of 5-, 6- and 7-cyanobiphenyl

E. M. Monge, J. Bryant[+], B. Obradovic[+], A. Harsono and A. J. Bain[*]

Department of Physics and Astronomy, University College London, London WC1E 6BT, UK
[+]Solexa Ltd, Chesterfield Research Park, Little Saffron Walden, Essex CB10 1XL,UK.

ABSTRACT

Picosecond fluorescence anisotropy and lifetime measurements are used to investigate the orientational dynamics and steady state order of the fluorescent probe oxazine 4 in the nematic and isotropic phases of 5, 6 and 7 cyanobiphenyl. Variation of the excitation polarisation angle β with respect to the nematic director allows the preparation of both cylindrically symmetric and asymmetrically aligned probe distributions whose relaxation dynamics are sensitive to both θ and ϕ motions yielding two characteristic relaxation times: τ_{20} (pure θ-diffusion) and τ_{22} (predominantly ϕ-diffusion). Analysis of the fluorescence intensity decays for excitation polarisation angles of $\beta=0°$ and $\beta=54.7°$ allows a determination of the effect of local field and differential reflection losses without the measurement of sample refractive indices. A striking feature of oxazine 4 dynamics in the approach to the nematic–isotropic phase transition temperature (T_{NI}) is that whilst θ diffusion shows a characteristic Arrhenius temperature dependence, the rate of diffusion in the ϕ co-ordinate is reduced as the system becomes less ordered. In the isotropic phase over a 50°C temperature range above T_{NI} the fluorescence anisotropy is characterised by two correlation times consistent with restricted rotational diffusion (intra-domain relaxation τ_f) within a slowly relaxing (pseudo-domain) structure (τ_s). The temperature dependence of τ_f and τ_s was in good agreement with recent theoretical models for intra- and inter-domain relaxation.

Keywords: Picosecond fluorescence polarisation, dye probe, liquid crystal, nematic phase, isotropic phase, orientational relaxation, order parameter, phase transition, oxazine 4.

1. INTRODUCTION

In an isotropic medium the relaxation of a molecular probe is necessarily independent of the choice of axis system with the consequence that θ and ϕ diffusion rates as measured in the laboratory frame are equivalent; however, in an ordered system this no longer holds[1]. Initial work in our group on probe diffusion in the nematic phase of 5CB indicated that θ and ϕ diffusion are strongly affected by the liquid crystal host with $\tau_{20} > \tau_{22}$[2,3]. Confinement of probe orientation in the θ co-ordinate (whilst ϕ remains globally unrestricted) was seen to give rise to highly restricted θ diffusion; this behaviour was observed across the nematic phase[1] with the equivalence in θ and ϕ recovered at T_{NI}. Models of isotropic phase dynamics have been based on a modification of the mean field phase transition theory introduced by de Gennes in the second order phase transition model developed by Landau[4]. Landau-de Gennes theory predicts the existence of local order over an interval above the nematic-isotropic (weakly first order) phase transition temperature T_{NI}. Experimental evidence for the existence of pseudo-domain structures over a significant temperature range in the isotropic phase has been provided by time domain dynamic light scattering in pure 5CB[5]. In the isotropic phase of 5CB the orientational diffusion of fluorescent probes, whilst yielding a zero steady state anisotropy was seen to depart from conventional single axis isotropic rotational diffusion (i.e. a single exponential decay). The fluorescence anisotropy was clearly bi-exponential and consistent with restricted rotational diffusion (τ_f) mediated by a slower overall rotational diffusion process (τ_s). An extension of these studies to both the nematic and isotropic phases of the higher cyanobiphenyls (6- and 7-CB) was therefore undertaken. Fluorescent probe studies in nematic liquid crystals are complicated by the effects of

---

Proceedings of SPIE Vol. 5213 Liquid Crystals VII, edited by Iam-Choon Khoo
(SPIE, Bellingham, WA, 2003) · 0277-786X/03/$15.00

213

optical anisotropy of the host (birefringence) and the anisotropic local field on emission intensities. Correction of fluorescence data is possible if refractive index data for the liquid crystal across the emission wavelength is known[2]. Extensive refractive index data for 5CB is available[6]. However, the extension of polarised photoselection experiments to liquid crystals where such data is unavailable required a new approach in which the anisotropy correction k was determined from an analysis of the fluorescence intensity decays for excitation polarisation angles of β=0° and 54.7°.

2. PHOTOSELECTION IN HIGHLY ALIGNED MEDIA

2.1 Single Photon Photoselection in Ordered Systems

The experimental arrangement for picosecond photoselection using variable linear polarisation is shown in figure 1 and has been described in detail elsewhere[7].
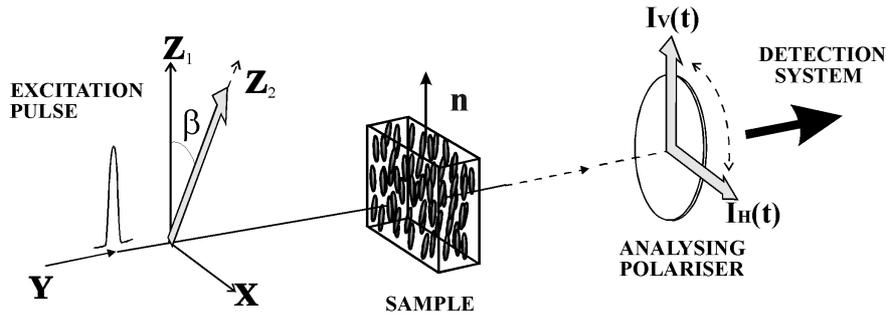

Figure 1: Schematic 180° excitation-detection experimental geometry utilising a variably polarised (β) excitation pulse. The excitation polarisation is varied with respect to the nematic director **n**. The V (Z) and H (X) polarised components of the probe emission intensity are built up using time –correlated single photon counting and used to construct the fluorescence anisotropy function R(t, β)

Irrespective of the excitation process, the measurement of fluorescence anisotropy from an arbitrarily ordered excited state is determined solely by the cylindrically symmetric and asymmetric degrees of molecular alignment. In the co-ordinate system (Z_1) of figure 1 the time-resolved fluorescence anisotropy is given by[1]

$$R(t) = \frac{I_V(t) - I_H(t)}{I_V(t) + 2I_H(t)} = \frac{\dfrac{\left\langle \alpha_{20}^{ex}(t) \right\rangle}{\sqrt{5}} - \dfrac{1}{\sqrt{30}}\left\{ \left\langle \alpha_{22}^{ex}(t) \right\rangle + \left\langle \alpha_{2-2}^{ex}(t) \right\rangle \right\}}{1 + \dfrac{2}{\sqrt{30}}\left\{ \left\langle \alpha_{22}^{ex}(t) \right\rangle + \left\langle \alpha_{2-2}^{ex}(t) \right\rangle \right\}} \tag{1}$$

where $\left\langle \alpha_{20}^{ex}(t) \right\rangle$ and $\left\{ \left\langle \alpha_{22}^{ex}(t) \right\rangle + \left\langle \alpha_{2-2}^{ex}(t) \right\rangle \right\}$ are the time-dependent cylindrically symmetric and asymmetric degrees of excited state alignment. Their initial values are dependent on the photoselection process and the degree of order in the ground state. The excitation polarisation angle β can be varied from 0˚ to 90˚ resulting in a transition probability of the form:

$$W_{abs}^{lab}(\theta,\phi,t) = B\frac{\sqrt{4\pi}}{3}\left[Y_{00}(\theta,\phi) + \frac{2}{\sqrt{5}}\sum_Q d_{Q0}^2(-\beta)Y_{2Q}(\theta,\phi) \right] \tag{2}$$

where B is a constant of proportionality. and $d_{Q0}^2(-\beta)$ is a reduced rotation matrix[8]. The initial moments of the excited state distribution are given by[1],

$$\left\langle C_{KQ}^{ex}(0) \right\rangle = \int\limits_0^{2\pi}\int\limits_0^{\pi} Y_{KQ}^*(\theta,\phi)W(\theta,\phi)P_{gs}(\theta,\phi)\sin\theta d\theta d\phi \tag{3}$$

With the expansion of the ground state distribution and insertion of (2) into (3) the single excited state moments become:

$$\left\langle C_{KQ}^{ex}(0) \right\rangle = B \frac{\sqrt{4\pi}}{3} \sum_{K'} \left\langle C_{K'0}^{gs}(ss) \right\rangle \left\langle KQ \middle| \left[Y_{00}(\theta,\phi) + \frac{2}{\sqrt{5}} \sum_{q} d_{q0}^2(-\beta) Y_{2q}(\theta,\phi) \right] \middle| K'0 \right\rangle \tag{4}$$

Evaluating matrix elements in (4) yields

$$\left\langle C_{KQ}^{ex}(0) \right\rangle = \frac{B}{3} \sum_{K'q} \left\langle C_{K'0}^{gs}(ss) \right\rangle \left[\delta_{K'K}\delta_{Q0} + \frac{2}{\sqrt{5}} d_q^2(-\beta) \begin{pmatrix} K & 2 & K' \\ -Q & q & 0 \end{pmatrix} \begin{pmatrix} K & 2 & K' \\ 0 & 0 & 0 \end{pmatrix} \sqrt{5}\hat{K}\hat{K}' \right] \tag{5}$$

The initial fluorescence observables are given by

$$\left\langle \alpha_{20}^{ex}(0) \right\rangle = \frac{\sum_{K'q} \left\langle C_{K'0}^{gs}(ss) \right\rangle \left[\delta_{K'2} + \frac{2}{\sqrt{5}} d_{0-q}^2(-\beta) \begin{pmatrix} 2 & 2 & K' \\ 0 & 0 & 0 \end{pmatrix}^2 \sqrt{5}\hat{K}\hat{K}' \right]}{\sum_{K'q} \left\langle C_{K'0}^{gs}(ss) \right\rangle \left[\delta_{K'0} + \frac{2}{\sqrt{5}} d_{0-q}^2(-\beta)\delta_{K'2} \right]} \tag{6}$$

$$\left\langle \alpha_{2\pm2}^{ex}(0) \right\rangle = \frac{\sum_{K'q} \left\langle C_{K'0}^{gs}(ss) \right\rangle \left[\frac{2}{\sqrt{5}} d_{0-q}^2(-\beta) \begin{pmatrix} 2 & 2 & K' \\ \mp 2 & q & 0 \end{pmatrix} \begin{pmatrix} 2 & 2 & K' \\ 0 & 0 & 0 \end{pmatrix} \sqrt{5}\hat{K}\hat{K}' \right]}{\sum_{K'q} \left\langle C_{K'0}^{gs}(ss) \right\rangle \left[\delta_{K'0} + \frac{2}{\sqrt{5}} d_{00}^2(-\beta)\delta_{K'2} \right]} \tag{7}$$

Insertion of (6) and (7) into (1) yields the initial fluorescence anisotropy in terms of the ground state order parameters and the excitation polarisation angle β. From the symmetry constraints of the 3j symbols it can be seen that only the K'=2 and 4 ground state order parameters contribute to the single-photon fluorescence anisotropy. Measurement of the initial single photon fluorescence anisotropy for excitation polarised parallel ($\beta = 0°$) and perpendicular to the nematic director ($\beta = 90°$) can thus be used to determine the K'=2 and 4 ground state order parameters. From (2) R(0, β) is thus

$$R(0,\beta) = \frac{\left[\frac{2}{5}\left(\cos^2\beta - \sin^2\beta\right) + \frac{\left\langle \alpha_{20}^{gs} \right\rangle}{\sqrt{5}}\left[1 + \frac{4}{7}\cos^2\beta \right] + \frac{\left\langle \alpha_{40}^{gs} \right\rangle}{35}\left(19\cos^2\beta - 7\right) \right]}{\left[1 + \frac{2}{5}\sin^2\beta + \frac{\left\langle \alpha_{20}^{gs} \right\rangle}{\sqrt{5}}\left[\frac{25\cos^2\beta - 11}{7} \right] + \frac{\left\langle \alpha_{40}^{gs} \right\rangle}{35}2\sin^2\beta \right]} \tag{8}$$

For $\beta = 0°$ the excitation process retains cylindrical symmetry about the laboratory Z-axis and the initial fluorescence anisotropy is characterised solely by the cylindrically symmetric excited state alignment. For $\beta=54.7°$ $\left\langle \alpha_{20}^{ex}(0) \right\rangle = \left\langle \alpha_{20}^{gs} \right\rangle$ irrespective of the relative values of $\left\langle \alpha_{20}^{gs} \right\rangle$ and $\left\langle \alpha_{40}^{gs} \right\rangle$. For linear orientational relaxation (where $\left\langle \alpha_{20}^{gs} \right\rangle$ and $\left\langle \alpha_{20}^{ex}(0) \right\rangle$ are equal or close), this excitation condition ensures that the time-dependent fluorescence anisotropy is dominated by the cylindrically asymmetric excited state alignment dynamics.

From symmetry considerations, the alignment relaxation dynamics in an ordered medium with cylindrical symmetry are of the form[1]

$$\left\langle \alpha_{20}^{ex}(t) \right\rangle = \left\{ \left\langle \alpha_{20}^{ex}(0) \right\rangle - \left\langle \alpha_{20}^{ex}(ss) \right\rangle \right\} \exp(-t/\tau_{20}) + \left\langle \alpha_{20}^{ex}(ss) \right\rangle$$

$$\left\{ \left\langle \alpha_{22}^{ex}(t) \right\rangle + \left\langle \alpha_{2-2}^{ex}(t) \right\rangle \right\} = \left\{ \left\langle \alpha_{22}^{ex}(0) \right\rangle + \left\langle \alpha_{2-2}^{ex}(0) \right\rangle \right\} \exp(-t/\tau_{22}) \tag{9}$$

where (*ss*) denotes the equilibrium or steady-state value of the probe alignment. The initial moments of the excited state distribution are given by equations (6) and (7) respectively. Substitution of equation (9) into these fluorescent observables and using equation (1) gives the time-dependent fluorescence anisotropy in terms of normalised excited state moments as:

$$R(t,\beta) = \frac{\left[\dfrac{(3\cos^2\beta - 1)}{35}\{7 + 6b\} + \dfrac{a}{7}(6\cos^2\beta + 5) - R_{ss}(1 + a(3\cos^2\beta - 1))\right]\exp(-t/\tau_{20})}{-\dfrac{1}{5}\sin^2\beta\left(1 - \dfrac{10}{7}a + \dfrac{b}{7}\right)\exp(-t/\tau_{22}) + R_{ss}(1 + a(3\cos^2\beta - 1))}{(1 + a(3\cos^2\beta - 1)) + \dfrac{2}{5}\sin^2\beta\left(1 - \dfrac{10}{7}a + \dfrac{b}{7}\right)\exp(-t/\tau_{22})} \tag{10}$$

where $a = \langle \alpha_{20}^{gs} \rangle / \sqrt{5}$ and $b = \langle \alpha_{40}^{gs} \rangle$.

2.2 Anisotropy Correction Factors

In a birefringent medium the vertical (V) and horizontally (H) polarised components of the fluorescence anisotropy are unequally affected by local field effects and reflection losses at the boundary between the sample and the cell wall[10,11]. Application of these considerations to emission from a molecular probe in a nematic host yields a dimensionless parameter; the anisotropy correction factor k (the change in $I_Z(t)/I_X(t)$ induced by these effects)[2,9],

$$k(\lambda,T) = \left(\frac{n_e}{n_o}\right)\left(\frac{n_o + n_g}{n_e + n_g}\right)^2\left(\frac{n_e^2 + 2}{n_o^2 + 2}\right) \tag{11}$$

where n_e and n_o are the extraordinary and ordinary refractive indices for the liquid crystal and n_g is the refractive index of the sample cell wall. The wavelength and temperature (λ,T) dependence of these quantities are well known for 5CB[6], however corrections must be made due to the shift in T_{NI} with the addition of the probe[2]. The extension of our studies to systems where refractive index data is not available and/or where the addition of molecular probes may have a significant influence on the optical and phase transition dynamics requires a different approach in which k can be determined independently in situ. We have shown recently that it is possible to determine k by a series of fluorescence lifetime and anisotropy measurements[9,12]. A second correction factor ($\bar{A}$) is necessary to account for the reduction in the fluorescence anisotropy from theoretical values due the possible contribution of a number of molecular and experimental factors. Principally these are the non-parallelism of absorption and emission transition dipole moments[1], depolarisation arising from sample concentration and path length effects[13] and depolarisation due to the collection optics. The $\bar{A}$ parameter is determined by the departure of the initial fluorescence anisotropy from its theoretical value in an isotropic sample[7]. For liquid crystalline media, the sample is raised to a few degrees above the nematic isotropic phase transition temperature where departure of R(0, β) from theory is then determined[12]. The values of $\bar{A}$ determined for oxazine 4 in 5-, 6- and 7-CB are 0.823, 0.923, 0.879, respectively. Finite values of k and $\bar{A}$ alter the relative contributions of the vertical and horizontally polarised fluorescence signals used to construct R(t) and to a reduction in the relative degrees of observed molecular alignment. The altered (observed) anisotropy (equation 10) becomes

$$R(t) = \frac{\dfrac{k-1}{\bar{A}} + \dfrac{(2k+1)}{\sqrt{5}}\left[\begin{array}{c}\left[\langle\alpha_{20}^{ex}(0)\rangle - \langle\alpha_{20}^{ex}(ss)\rangle\right]\exp(-t/\tau_{20}) \\ + \langle\alpha_{20}^{ex}(ss)\rangle\end{array}\right] - \dfrac{1}{\sqrt{30}}\{\langle\alpha_{22}^{ex}(0)\rangle + \langle\alpha_{2-2}^{ex}(0)\rangle\}\exp(-t/\tau_{22})}{\dfrac{k+2}{\bar{A}} + \dfrac{(2k-2)}{\sqrt{5}}\left[\begin{array}{c}\left[\langle\alpha_{20}^{ex}(0)\rangle - \langle\alpha_{20}^{ex}(ss)\rangle\right]\exp(-t/\tau_{20}) \\ + \langle\alpha_{20}^{ex}(ss)\rangle\end{array}\right] + \dfrac{2}{\sqrt{30}}\{\langle\alpha_{22}^{ex}(0)\rangle + \langle\alpha_{2-2}^{ex}(0)\rangle\}\exp(-t/\tau_{22})} \tag{12}$$

3. ORIENTATIONAL DYNAMICS IN ISOTROPIC BUT LOCALLY RESTRICTED ENVIRONMENTS

Studies of probe fluorescence anisotropy in (globally isotropic) biological systems such as cell membranes are characterised by a non-zero steady state anisotropy. This was explained in terms of the restricted rotational diffusion within a fixed or very slowly moving environment. The 'cone model'[14] has been widely used to interpret fluorescence anisotropy in such environments. Restricted rotational diffusion is modelled as diffusion or 'wobbling' within a cone defined by the angular limits $0 \leq \theta \leq \theta_{max}$ where θ_{max} is the maximum angle of the cone. Fluorescence emission is related to the motion of molecular fixed transition dipole moments within the local environment, which is taken to remain static. The extension of this approach to systems where the isotropic diffusion of the local environment is on a longer timescale is straightforward providing the two diffusive processes are uncorrelated[15]. The overall rotational correlation function can be described in terms of a product of the two individual correlation functions, giving rise to two independent rotational relaxation times

$$R(t) = R(0)\left[(1-F)\exp\left(-t/\tau_f\right) + F\right]\exp\left(-t/\tau_s\right) \tag{13}$$

$R(0)$ represents the global initial anisotropy, τ_f is the relaxation time for the probe rotation within the local environment (the cone) and τ_s is the reorientational time for overall isotropic rotational diffusion of the domain. For parallel absorption and emission transition dipole moments, F is given by:

$$F = \left[0.5\cos\theta_{MAX}\left(1+\cos\theta_{MAX}\right)\right]^2 \tag{14}$$

4. EXPERIMENTAL REALISATION

A schematic representation of the experimental apparatus is shown in figure 1. The oxazine 4 doped (c.a. 10^{-4}M) nematic n-CB (n = 5, 6, 7) was held in 100μm thick quartz cells. The cell walls were spin-coated with a surfactant (polyvinyl alcohol solution) and rubbed mechanically to create a homogeneous liquid crystal alignment. Fluorescence collection and analysis utilised a collinear geometry with respect to the normally incident Z-polarised excitation pulse (615nm, 7ps). Fluorescence was detected and recorded using a time-correlated single photon counting[7]. The temperature was varied and monitored over the nematic range of both liquid crystals using a precision temperature controlled oven (±0.1°C). Vertical (I_V) and parallel (I_H) intensities for the excitation polarisation angles β=0°, 54.7° and 90° were recorded over this temperature range by gradually increasing the temperature in small steps. Construction of the R(t, β) decays from I_V and I_H measurements (see equation (2)) was carried out using a MicroCal Origin graphic software package. Typical results for oxazine 4 in 7CB at T = 30°C are shown in figure 2.

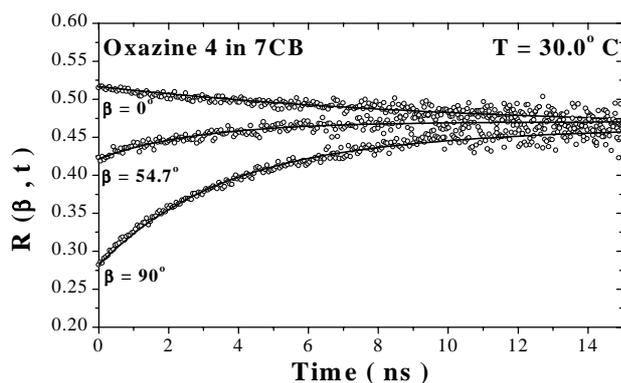Figure 2: (a) Anisotropy decays measured for oxazine 4 in 4-heptyl-4'-cyanobiphenyl (7CB) by varying the excitation polarisation angle (β=0°, 90° and 54.7° (magic angle)) at a fixed temperature of 30.0±0.1°C. Solid lines correspond to least squares fits to the data.

4.1 Anisotropy Correction Factor

In a cylindrically symmetric medium, measurement of the total fluorescence intensity I_V+2I_H yields a fluorescence signal that contains solely population terms. However, in the presence of sample birefringence and local field effects the total intensity for Z-polarised excitation ($\beta=0°$) is given by[9]

$$I_V + 2I_H(\beta = 0^o) = A\exp\left(-t/\tau_f\right)\left[\frac{k+2}{\bar{A}} + \frac{2(k-1)}{\sqrt{5}}\left\{\left[\left\langle\alpha_{20}^{ex}(0)\right\rangle - \left\langle\alpha_{20}^{ex}(ss)\right\rangle\right]\exp(-t/\tau_{20}) + \left\langle\alpha_{20}^{ex}(ss)\right\rangle\right\}\right] \tag{15}$$

where A is a proportionality constant. In the nematic phase $k>1$ and the normally vanishing alignment term in (15) will make a small contribution to the signal. For magic-angle excitation ($\beta=54.7°$) the vertically polarised component of the fluorescence intensity has no k dependence and the initial alignment produced is equal to that of the ground state distribution[1] the fluorescence intensity is thus,

$$I_Z(\beta = 54.7^o) = A'\exp\left(-t/\tau_f\right)\left[\frac{1}{\bar{A}} + \frac{2}{\sqrt{5}}\left(\left\{\left\langle\alpha_{20}^{gs}(0)\right\rangle - \left\langle\alpha_{20}^{ex}(ss)\right\rangle\right\}\exp(-t/\tau_{20}) + \left\langle\alpha_{20}^{ex}(ss)\right\rangle\right)\right] \tag{16}$$

where A' is a constant of proportionality. Given a small (or zero) alignment difference between the ground and excited state equilibrium degrees of alignment (16) should yield a single exponential decay with a lifetime τ_f. Comparison of the two intensity decays corresponding to (15) and (16) allows k to be determined.
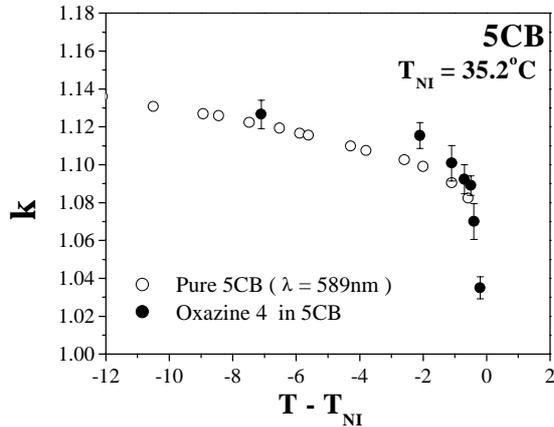

Figure 3: Variation in the anisotropy correction factor k with reduced temperature. Open circles correspond to k values calculated from literature refractive index data for neat 5CB at 589nm. Closed symbols correspond to values of k obtained for oxazine 4 doped 5CB using the comparison of intensity decays for β= 0°and 54.7°.

4.2 Determination of Ground State Order Parameters and Excited State Rotational Dynamics

Taking account of the influence of k and $\bar{A}$ (10) becomes

$$R\left(t,\beta = 0^o\right) = \frac{(1+2a)\dfrac{(k-1)}{\bar{A}} + (2k+1)\left(\left\{\left[\dfrac{2}{5} + \left(\dfrac{11}{7}\right)a + \dfrac{36}{35}b\right] - R_{SS}\right\}\exp(-t/\tau_{20}) - R_{SS}\right)}{(1+2a)\dfrac{(k+2)}{\bar{A}} + 2(k-1)\left(\left\{\left[\dfrac{2}{5} + \left(\dfrac{11}{7}\right)a + \dfrac{36}{35}b\right] - R_{SS}\right\}\exp(-t/\tau_{20}) - R_{SS}\right)} \tag{17}$$

Analysis of the initial fluorescence anisotropies for $\beta=0°$ and $\beta=90°$ yields, with the input of k and $\bar{A}$, the values of the K=2 (a) and K=4 (b) ground state order parameters. With this information it is possible to analyse the $\beta=0°$ excited fluorescence anisotropy to determine an accurate value for τ_{20}. A non-linear least squares fit to the $R(t,\beta=0°)$ data to equation (17) yields τ_{20} and R_{SS}. For an excitation polarisation angle of $\beta=90°$, the cylindrically asymmetric alignment contribution (ϕ-diffusion) to the fluorescence anisotropy is maximised[1] (see figure 2) and the fluorescence anisotropy has the form:

$$R\left(t, \beta = 90^\circ\right) = \frac{(1-a)\frac{(k-1)}{\bar{A}} + (2k-1)\left(\left\{\left[-\frac{1}{5} + \frac{5a}{7} - \frac{18b}{35}\right] - R_{ss}\right\}\exp(-t/\tau_{20}) + R_{ss}\right) - \frac{1}{5}\left[1 - \frac{10a}{7} - \frac{3b}{7}\right]\exp(-t/\tau_{22})}{(1-2a)\frac{(k+2)}{\bar{A}} + 2(k-1)\left(\left\{\left[-\frac{1}{5} + \frac{5a}{7} - \frac{18b}{35}\right] - R_{ss}\right\}\exp(-t/\tau_{20}) + R_{ss}\right) + \frac{2}{5}\left[1 - \frac{10a}{7} - \frac{3b}{7}\right]\exp(-t/\tau_{22})} \quad (18)$$

A least squares fit to (18) using the values of k, $\bar{A}$, a, b and τ_{20}, obtained as detailed above, allows the cylindrically asymmetric relaxation time τ_{22} to be determined.

4.3 Fluorescence Anisotropy in the Isotropic Phase

In the isotropic phase, k is necessarily unity and there is no distinction between θ and ϕ diffusion in the laboratory frame. Fluorescence anisotropy decays for a single excitation polarisation ($\beta=0^\circ$) were recorded, initial anisotropy measurements were as a function of β were however recorded close to the phase transition temperature to determine $\bar{A}$. R(t, $\beta=0^\circ$) measurements were analysed using (13).

5. RESULTS

5.1 Ground State Order Parameters

Measurements of the initial fluorescence anisotropies of oxazine 4 for excitation polarisation angles of $\beta=0^\circ$ and 90° yielded values of the K=2 and K=4 moments of the ground state probe distribution functions in 5-, 6- and 7 cyanobiphenyl. Experimentally determined values of $\left\langle\alpha_{20}^{gs}\right\rangle$ and $\left\langle\alpha_{40}^{gs}\right\rangle$ do not yield a complete distribution function and the inclusion of higher moments is necessary[2, 16,17]. The direct determination of higher moments in the ground state distribution function is not possible using single photon excitation[1, 17]. However, it is possible to make physically reasonable estimates for the 'missing' moments[11]. With the sole constraint that the distribution retains a single maximum between 0° and 90°, trial values for the higher (K = 6, 8, 10 and 12) moments are added sequentially in decreasing magnitude such that the ground state distribution function remains positive. The validity of this approach has been recently confirmed using two and single photon fluorescence anisotropy measurements[17]. Using this approach for oxazine 4 in the three nematic hosts, the resulting distribution functions are well approximated by Gaussian distributions centred about a peak angle θ_{MAX} as can be seen for oxazine 4 in 7CB at 42.6^{o}C in figure 4.
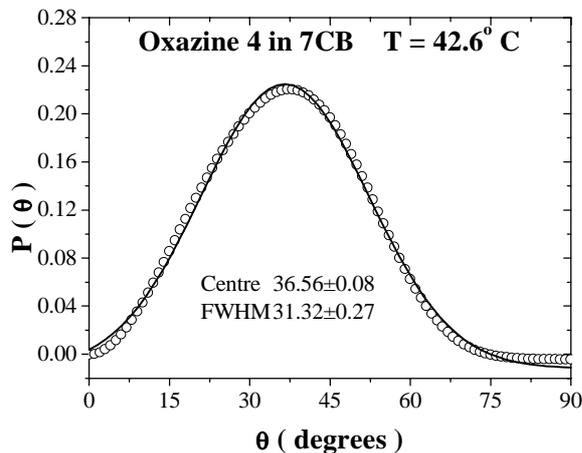

Figure 4: The orientational distribution function P(θ) for oxazine 4 in 7CB at 42.6^{o}C. The solid line represents a Gaussian fit to the data giving a maximum at 36.56^o±0.08^o and a FWHM of 31.32^o±0.27^o.

Variation in the peak angle (θ_{MAX}) of the ground state distribution functions of oxazine 4 across the nematic temperature range of 5, 6 and 7 cyanobiphenyl is shown in figure 5(a). The peak angle θ_{MAX} is found to vary between 31.5° and 40° across the nematic temperature range of the three cyanobiphenyls; the values and variation in θ_{MAX} with reduced temperature (T-T_{NI}) are closely reproduced in each nematic host. There is an approximately linear increase with

temperature (c.a. 0.3°/°C) up to c.a.1-2 °C of T_{NI}. At this point there is a sharp increase in θ_{MAX} of 4-6° before each system becomes globally isotropic. It is notable that through the entire nematic temperature range oxazine 4 is oriented at an angle less than θ_{ALKYL}. The distribution functions obtained for oxazine 4 are consistent with their adoption of sites of comparable symmetry and orientation within the nematic host. Cyanobiphenyl molecules are known to be ordered in a 'head to tail' configuration as illustrated in figure 5(b)[11]. The elimination of one cyanobiphenyl dimers allows the formation of a pocket of approximately the correct symmetry and volume for the oxazine probe molecule to occupy[12] (see figure 5b).
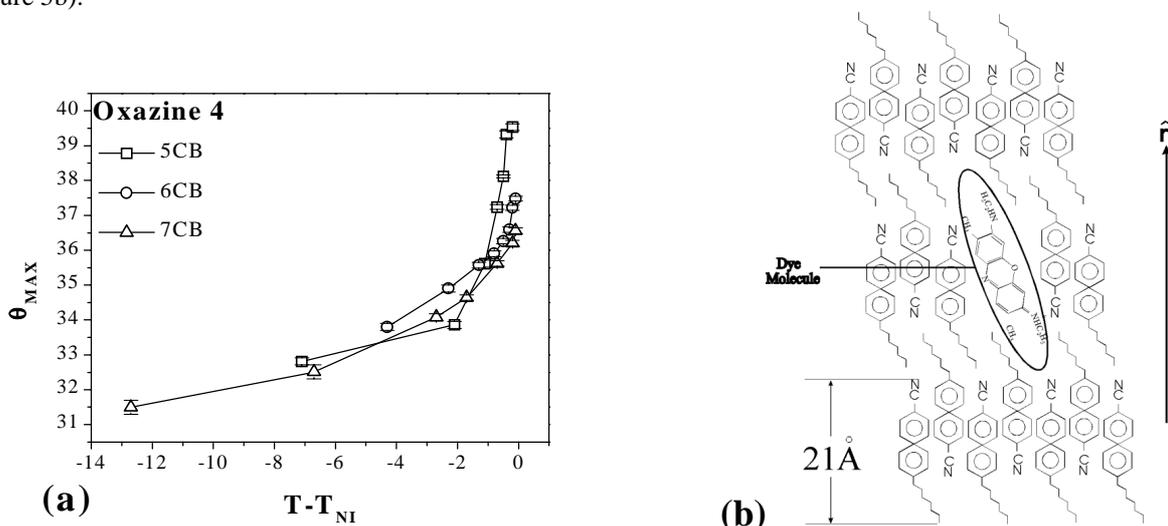

Figure 5a: Variation in θ_{MAX} as a function of the reduced temperature for oxazine 4 in 5-, 6- and 7CB. 5b: Illustration of the 'pocket' between the alkyl tails formed by the elimination of one 7CB dimer close to the orientation of oxazine 4 with respect to the nematic director and the alkyl tail orientation.

5.2 Orientational Dynamics

Assuming that the orientational dynamics are dominated by anisotropic friction, the small θ dependence present in τ_{22} can be removed to yield a pure ϕ diffusion time[1,7]. The temperature variation in τ_θ and τ_ϕ for oxazine 4 diffusion in 5, 6 and 7CB is shown in figure 6. It is clear from the results that the departure from isotropic orientational relaxation dynamics ($\tau_\theta = \tau_\phi$) is marked across the nematic range of the three hosts $\tau_\theta > \tau_\phi$. This difference is most marked in 5CB where $\tau_\theta \cong 8\tau_\phi$ at c.a. 7°C from T_{NI}. The temperature dependence of the two rotational correlation times is perhaps the most striking feature of the departure from isotropic rotational diffusion; τ_θ decreases with increasing temperature, in agreement with previous observations of Arrhenius behaviour for θ-diffusion in the nematic phase[18]. The temperature dependence for ϕ diffusion is wholly different; τ_ϕ shows little temperature variation across the nematic phase but *increases* with temperature within 1-2°C of T_{NI}. The differences in τ_θ and τ_ϕ must arise from differences in the effective friction (i.e. viscosity) experienced by θ and ϕ motions of the probe. Oxazine 4 is seen to correlate strongly with the order of the liquid crystal host. Under these circumstances, the rotational diffusion of the probe should exhibit a similar asymmetry to that of the nematic host in which the bulk viscosity is highly anisotropic[19]. A slowing of the molecular spinning rate with increasing temperature has been inferred from changes in Raman band shapes for the nematic phase of pure OET[20]. This behaviour was qualitatively attributed to a breakdown in local cylindrical symmetry in the vicinity of the nematic-isotropic phase transition. The breakdown in cylindrical symmetry giving rise to so-called "biaxial fluctuations" due to the uncorrelated motion of different segments (tails) of individual nematogens whose interference acts to increase the friction (viscosity) experienced for ϕ diffusion. Evidence for an increase in viscosity in the approach to T_{NI} is provided by recent measurements of translational (mass) diffusion in pure[21] and dye doped cyanobiphenyls[22].
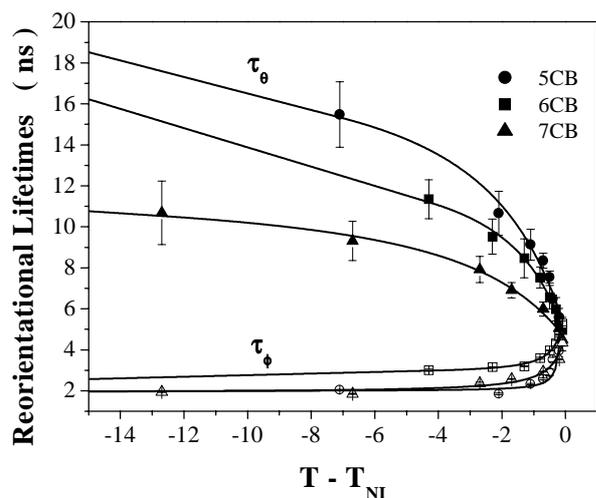
Figure 6: Variation in the θ and φ diffusion times for oxazine 4 with reduced temperature in the nematic phases of 5-, 6-, and 7-CB.

5.3 Isotropic Phase Dynamics

Measurements of single photon fluorescence anisotropy in the isotropic phase of 5, 6 and 7CB were undertaken in aligned dye doped (5×10^{-4} M) cells prepared as outlined in section 4 for temperatures close to, and above, the nematic temperature. Within a temperature region extending from T_{NI} to c.a. $T_{NI}+50°C$ all oxazine 4 fluorescence anisotropies were well described by (13). The variation in τ_f and τ_s with temperature in the isotropic phases of 5, 6 and 7 cyanobiphenyl is shown in figure 7.
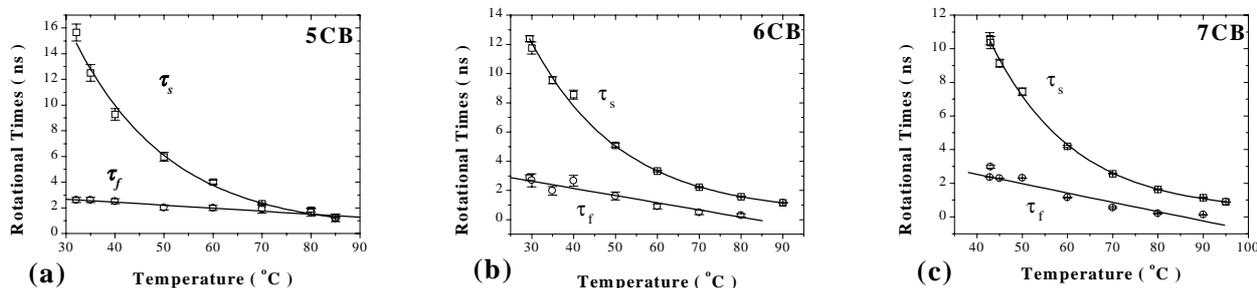

Figure 7: Temperature dependence of the fast and slow orientational relaxation times for oxazine 4 in 5CB (a), 6CB(b) and 7CB(c).

The variation of the slow (inter-domain) rotational time with temperature can be related to the temperature dependent shear viscosity of the liquid crystal in the isotropic phase[23]

$$\tau_S \approx \frac{\eta(T)V_{eff}}{k_B\left(T-T^*\right)} + \tau_0 \tag{19}$$

where V_{eff} is the hydrodynamic volume of the dye molecule, τ_0 is the free rotor correlation time (the reorientation time at zero viscosity[24]) and k_B is the Boltzmann constant. A linear dependence representation of the slow reorientational rotational time with $\eta(T)/(T-T^*)$ predicted by (19) was observed for all three cyanobiphenyls. Values of V_{eff} varied between 249Å^3 and 303Å^3 in reasonable agreement with the Van der Waals calculation of 283Å^3 for oxazine 4. The fast (intra-domain) probe diffusion time follows a linear decrease with temperature (see figure 6). This behaviour is in

accordance with density functional predictions for "intermediate-time" relaxation dynamics (of the order of nanoseconds) in liquid crystals[25] where the relaxation time dependence on viscosity and temperature is given by:

$$\tau_f \approx \frac{\eta V_{eff}}{k_B T} \qquad (20)$$

Fits to the data using (20) are shown in figure 6. At temperatures approaching 90°C the domain structure apparently collapses, a single exponential decay time for the anisotropy is recovered as is observed for oxazine 4 diffusion in non-mecogenic cyanobiphenyls such as 3CB[12]. The temperature variation of the full angular width of the oxazine 4 distributions, in both the nematic and isotropic phases of 5, 6 and 7CB is shown in figure 8. Across the phase transition temperature there is clear evidence of a discontinuity (a small "jump") in the angular width of the probe characteristic of a weak first order phase transition[4].
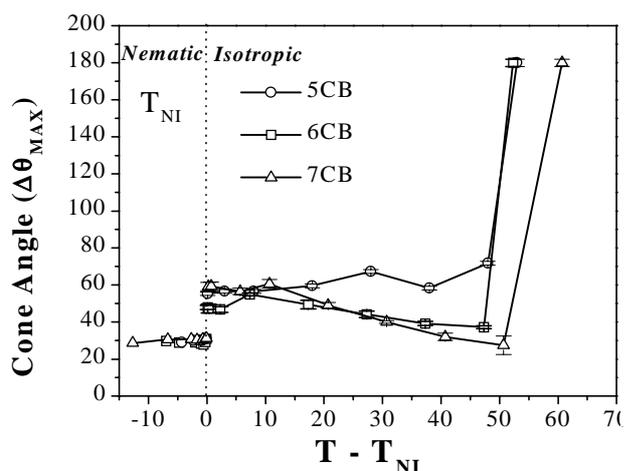

Figure 7: Temperature variation in the width of the angular distribution of oxazine 4 across the isotropic and nematic phases of 5-, 6- and 7CB. The cone angle values obtained from (14) correspond to the half width of the angular distribution and have been doubled to permit a comparison with the Gaussian widths of the nematic phase distributions.

In 6 and 7CB, oxazine 4 shows a consistent decrease in the angular width with temperature until c.a. 50°C above T_{NI}. At this point, there is a rapid collapse to a wholly isotropic environment. In contrast, for 5CB a slow overall increase in $\Delta\theta_{max}$ is observed. An explanation of this anomalous behaviour is not immediately apparent; an increase in local order with increasing temperature would appear counter intuitive. Oxazine 4 closely mirrors the order and dynamical behaviour of the three cyanobiphenyl hosts in the nematic phase. Entanglement of the alkyl tails has been proposed as possible mechanism for the observed reductions in τ_θ in the approach to the isotropic transition. The small change in the cone angle (angular width of the local environment) of oxazine 4 at T_{NI} is constrained by a value of $\Delta\theta_{max}$ (c.a. 60°) in the isotropic phase. It is possible that further alkyl tail entanglement persists in the nematic phase, which in the case of 6- and 7CB may lead to further restrictions in local motion of the probe.

6. CONCLUSIONS

We have successfully undertaken the first direct and detailed time resolved measurements of the full angular motion (θ and ϕ diffusion) and order of fluorescent probes in highly aligned optically anisotropic media. Using a range of excitation polarisations it has been possible to determine anisotropy correction factors within the course of the experiment, without the need to make detailed refractive index measurements, allowing accurate studies of probe dynamics to be extended to any highly ordered system with axial symmetry. Oxazine 4 dynamics are seen to depart considerably from isotropic rotational diffusion in both the nematic and isotropic phases of 5-, 6- and 7CB with the fluorophore constrained within a local environment. Hence, rotational diffusion with respect to the (global) nematic director is highly anisotropic with τ_θ significantly larger than τ_ϕ. The reduction in the ϕ diffusion rate (τ_ϕ^{-1}) with temperature in the vicinity of T_{NI} is the first direct observation of decreasing angular diffusion (and hence increasing

viscosity) in the approach to the nematic–isotropic phase transition. Significant retention of local order in the oxazine 4 is retained into the isotropic phase with inter and intra-domain probe relaxation times that are in good agreement with the predictions of recent theory.

ACKNOWLEDGEMENTS

REFERENCES

[1] A J Bain, P Chandna, and J Bryant, J. Chem. Phys. **112**, 10418-10434 (2000)

[2] J Bryant, Ph.D. thesis, University of Essex (2000)

[3] D A Armoogum, J Bryant, E M Monge and A J Bain, Proc. SPIE **4799**, 63-73 (2002)

[4] P G de Gennes and P Prost, *The Physics of Liquid Crystals* (2nd Ed.), Clarendon Press, Oxford (1993)

[5] F W Deeg and M D Fayer, J. Chem. Phys. **91**, 2269-2279, (1989)

[6] S T Wu and C S Wu, Opt. Eng., **32**(8), 1775-1781, (1993)

[7] A J Bain, P Chandna, G Butcher and J Bryant, J. Chem. Phys. **112**, 10435-10449 (2000)

[8] D M Brink and G R Satchler, *Angular Momentum* (3rd ed), Oxford Science (1993)

[9] A J Bain, D A Armoogum J Bryant and E M Monge, to be published

[10] I I Penvhev, I N Dozov, Mol. Cryst. Liq. Cryst. **73**, 267-271 (1981)

[11] S D Durbin and Y R Shen, Phys. Rev. A. **30**(3), 1419-1429 (1984)

[12] E M Monge, Ph. D. thesis, University of London (2003)

[13] P R Hammond, J. Chem. Phys. **70**, 3884-3894 (1979)

[14] K Kinosita, S Kawato and A Ikagami, Biophys. J. **20**, 289-295, (1977)

[15] C Zannoni, A Arcioni and P Cavatorta, Chem. Phys. Lip **32**, 179-250, (1983)

[16] E M Monge, D A Armoogum and A J Bain, Proc. SPIE **4797**, 264-274 (2002)

[17] A J Bain in *An Introduction to Laser Spectroscopy*, (D L Andrews and A Demidov, eds.) pp 171-210, Kluwer Scientific, London (2002)

[18] A Arcioni, F Bertinelli, R Tarroni and C Zannoni, Molecular Physics, **61**(5), 1161-1169 (1987)

[19] E Ciampi, J W Emsley, G R Luckhurst and B A Timimi, J. Chem. Phys. **107**, 5907-5913, (1997)

[20] M P Fontanta, B Rosi and N Kirov, Phys. Rev. Lett. **56**, 1708-1711, (1986)

[21] S V Dvinskikh, I Furo, H Zimmermann and A Maliniak, Phys. Rev. E. **65**, 061701 1-9, (2002)

[22] D R Spiegel, A L Thompson and W C Campbell, J. Chem. Phys. **114**, 3842-3847, (2001)

[23] R Torre, F Tempestini, P Bartolini and R Righini, Philos. Mag. B, **77**(2), 645-653, (1998)

[24] R M Anderton and J F Kauffman, J. Phys. Chem. **98**, 12117-12124, (1994)

[25] B Bagchi, J. Chem. Phys. **115**, 2207-2211, (2001)